



Genetic and Population Analysis

A Sparse Graph-structured Lasso Mixed model for genetic association with confounding correction

Wenting Ye^{1,*}, Xiang Liu², Tianwei Yue¹ and Wenping Wang¹¹School of Computer Science, Carnegie Mellon University, Pittsburgh, PA 15213, USA and²School of Computing, National University of Singapore, Singapore 119077

*To whom correspondence should be addressed.

Associate Editor:

Received on XXXXX; revised on XXXXX; accepted on XXXXX

Abstract

Motivation: While linear mixed model (LMM) has shown a competitive performance in correcting spurious associations raised by population stratification, family structures, and cryptic relatedness, more challenges are still to be addressed regarding the complex structure of genotypic and phenotypic data. For example, geneticists have discovered that some clusters of phenotypes are more co-expressed than others. Hence, a joint analysis that can utilize such relatedness information in a heterogeneous data set is crucial for genetic modeling.

Results: We proposed the sparse graph-structured linear mixed model (sGLMM) that can incorporate the relatedness information from traits in a dataset with confounding correction. Our method is capable of uncovering the genetic associations of a large number of phenotypes together while considering the relatedness of these phenotypes. Through extensive simulations and real data experiments, we show that the proposed model outperforms other existing approaches.

Availability: Source code and test data are freely available at <https://github.com/YeWenting/sGLMM>

Contact: wentingye52@gmail.com

1 INTRODUCTION

The recent years have witnessed a substantial advance in the exploration of the genetic architecture and linkage mapping between genetic markers and phenotypes. The advance of genome-wide association studies (GWAS) has helped scientists to discover genetic variants that are potentially causal to complex diseases (Kim *et al.*, 2015; Wang *et al.*, 2015), such as the evaluation of human diseases like type 2 diabetes (Craddock *et al.*, 2010), comprehending evolutionary patterns (Kruuk, 2004) and assisting animal breeding programs (Meyer *et al.*, 2004).

However, identifying the genetic variants is still a challenging task. The most important feature of GWAS is their sheer scale. Hundreds of thousands of SNPs (single nucleotide polymorphisms) are now being typed on samples involving thousands of individuals. With the number of predictors far exceeding the number of observation, it's nearly impossible to employ the classical multivariate regression. Hence geneticists have to opt for simple univariate linear regression that analyzes one SNP at a time (McCarthy *et al.*, 2008). Given that most of the complex traits are

polygenic, this apparently amounts to the model misspecification, resulting in false discovery whenever a lack of independence between loci (such as population structure) occurs (Hoggart *et al.*, 2008; Price *et al.*, 2010; Kang *et al.*, 2010).

Since the traditional methods are not expected to explain most of the genetic variations (Visscher *et al.*, 2012), biologists have developed many approaches to analyze polygenetic effects (Wu *et al.*, 2009; Logsdon *et al.*, 2010; Yang *et al.*, 2010). The most popular method is ℓ_1 -norm regularization (i.e. lasso regression) (Tibshirani, 1996). Recent studies have extended the model capability by adding different regularizers (Fan and Li, 2012), such as the smoothly clipped absolute deviation (SCAD) (Fan and Li, 2001) and the minimax concave penalty (MCP) (Zhang *et al.*, 2010a), which improve the performance by introducing non-smooth penalty in the optimization problem. However, the above-mentioned methods ignore the prolific dependency information between responses, as shown in the Figure 1b. Chen *et al.* (2010) proposed graph-structured regression method (GFlasso) that can incorporate such information through a given correlation graph.

On the other hand, confounders like population structure will induce the spurious associations between the genotypes and phenotypes, caused

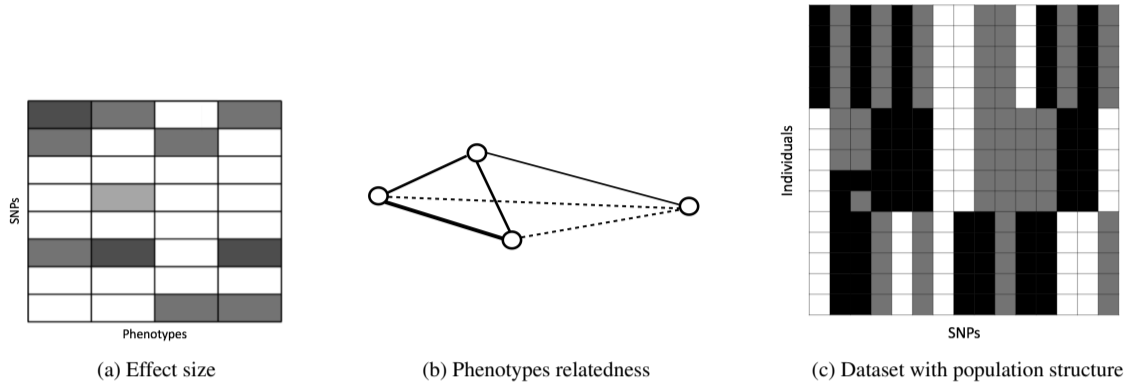


Fig. 1. An illustration of phenotypes relatedness and population structure as a confounding factor. (a): The sparse and correlated phenotypic structure with white entries for zeros and gray entries for nonzero values. (b): The phenotypes relatedness graph corresponding to panel (a) with solid line for strong correlation and dotted line for weak correlation. It’s clear that the three of the phenotypes have the strong connection between each other. (c): The dataset with population structure. The samples are originated from three populations and individuals from the same population tend to share common SNPs.

by the deviation from the idealized i.i.d. assumption in statistics. We demonstrate this issue in the Figure 1a and Figure 1c. Consequently, naïvely applying classic linear regression will lead to a substantial amount of false positive discoveries (Astle and Balding, 2009). Two popular approaches to address this is principal components analysis (PCA) (Price *et al.*, 2006; Patterson *et al.*, 2006) and linear mixed models (Goddard, 2009; Kang *et al.*, 2010). There is an increasing number of models proposed based on LMM due to the improvements that allow their application to human-scale genome data (Lippert *et al.*, 2011; Pirinen *et al.*, 2013). The FaST-LMM-Select improves its performance by selecting a small number of SNPs systematically (Listgarten *et al.*, 2012). The BOLT-LMM requires fewer iterations and increases power by modeling more realistic, non-infinitesimal genetic architectures (Loh *et al.*, 2015). The liability-threshold mixed linear model overcomes the LMM’s limitation in case-control ascertainment (Hayeck *et al.*, 2015). Wang *et al.* (2022) recently studies the statistical properties and different tradeoffs when applying mixed models in GWAS.

There have been several attempts to employ confounding correction and linkage mapping jointly (Bondell *et al.*, 2010; Fan and Li, 2012; Wang and Yang, 2016; Liu *et al.*, 2017; Wang *et al.*, 2019; Dinga *et al.*, 2020; Hatoum *et al.*, 2020). Segura *et al.* have proposed a related multi-locus mixed model using step-wise forward selection (Segura *et al.*, 2012). In parallel to our work, Rakitsch *et al.* (2013) introduced a model called lasso multi-marker mixed model (sLMM) to solve this problem but only considering one single trait. Korte *et al.* (2012) extended the ability of LMM to carry out GWAS on correlated phenotypes. However, the proposed approach requires setting parameters for each pair of traits, and hence cannot scale to the large dataset.

In this article, we extend the recent solutions of sparse linear mixed model that can correct confounding factors and perform genetic association simultaneously further to account the relatedness between different traits. We propose a new-fashioned analysis method, named sparse graph-structured linear mixed model (sGLMM), that can reconstruct the convoluted phenotypic architecture in a dataset originated from different populations. The proposed model requires no prior knowledge of the individual relationship and is capable of learning the structured pattern in a way that is properly calibrated to the degrees of traits’ relatedness.

The rest of the paper is organized as follow. In Section 2, we introduce a novel method to accomplish both structured genetic association and confounding correction simultaneously. In Section 3, through extensive

simulation experiments, we show the superiority of the proposed model in finding active SNPs. Then in Section 4 sGLMM is validated in the real-world genomic dataset from two different species and the discovered knowledge is discussed.

2 Method

In this section, the framework of the sparse linear mixed model will be introduced first. Then we propose the sparse graph-structured linear mixed model to extend sLMM by taking the relatedness between traits into consideration.

2.1 Sparse linear mixed model

Assume that data are collected for m SNPs and k phenotypes over n individuals. Let a $n \times m$ matrix \mathbf{X} denote the covariates, genotypes of each individual, and a $n \times k$ matrix \mathbf{y} stand for responses, traits of each individual. For each phenotype, we assume a standard liner mixed model as Equation 1:

$$\mathbf{y}_i = \mathbf{X}\boldsymbol{\beta}_i + \mathbf{u}_i + \boldsymbol{\epsilon}_i \quad (1)$$

where $\boldsymbol{\beta}_i$ is a $m \times 1$ vector for i -th trait’s fixed effect, \mathbf{u}_i for random effect and $\boldsymbol{\epsilon}_i$ for observation noise. Both \mathbf{u}_i and $\boldsymbol{\epsilon}_i$ are $n \times 1$ vectors. Throughout this paper, we use subscripts to denote columns and superscripts to denote rows, for example, $\boldsymbol{\beta}_i$ and $\boldsymbol{\beta}^i$ are the i -th column and i -th row of $\boldsymbol{\beta}$ respectively, and $\boldsymbol{\beta}$ stands for the whole effect size matrix.

\mathbf{u}_i and $\boldsymbol{\epsilon}_i$ are random variables with zero means, while having different covariances. The \mathbf{u}_i cannot be observed in a straight way, nonetheless, there are many avenues to obtain its covariance matrix \mathbf{K} . One is to employ the realized relationship matrix (RRM), a measure of genetic similarity to get the probabilities that pairs of individuals have causative alleles in common (Goddard *et al.*, 2009; Hayes *et al.*, 2009; Yang *et al.*, 2010). Marginalizing over the random effect \mathbf{u}_i will lead to a Gaussian marginal likelihood model (Kang *et al.*, 2008). Assuming that \mathbf{u}_i and $\boldsymbol{\epsilon}_i$ follow the Gaussian distribution with covariance $\sigma_g^2\mathbf{K}$ and $\sigma_e^2\mathbf{I}$ respectively, we can conclude that:

$$\mathbf{y}_i \sim \mathcal{N}(\mathbf{X}\boldsymbol{\beta}_i, \sigma_g^2\mathbf{K} + \sigma_e^2\mathbf{I}) \quad (2)$$

Assuming the priori distribution of $\boldsymbol{\beta}$ could be expressed as $e^{-\Phi(\boldsymbol{\beta})}$, we can define the likelihood function of the linear mixed model as:

$$\ell(\sigma_g^2, \sigma_\epsilon^2, \boldsymbol{\beta}) = e^{-\Phi(\boldsymbol{\beta})} \cdot \prod_{i=1}^k \mathcal{N}(\mathbf{y}_i | \mathbf{X}\boldsymbol{\beta}_i, \sigma_g^2 \mathbf{K} + \sigma_\epsilon^2 \mathbf{I}) \quad (3)$$

To accord with the reality that the majority of SNP's effect size are zero, sLMM assumes that $\boldsymbol{\beta}$ follows Laplace shrinkage prior, and the resulting $\Phi(\boldsymbol{\beta})$ could be written as Equation 4:

$$\Phi(\boldsymbol{\beta}) = \lambda \|\boldsymbol{\beta}\|_1 \quad (4)$$

Where $\|\cdot\|_1$ denotes the entry-wise matrix ℓ_1 -norm and λ controls the overall sparsity. As increasing λ , the fewer active genetic variants will be yielded. Substitute this penalty into Equation 3, we can get the sparse linear mixed model. However, this lasso penalty fails to consider the relatedness between different traits. Such defect drives us to the sparse graph-structured linear mixed model.

2.2 Sparse graph-structured linear mixed model

Based on the framework in Equation 3, we introduce the graph-fusion penalty to model the dependency between different traits. Given a graph G with a set of nodes $V = \{1, \dots, k\}$ and weighted edges E . The weight of the edge determines the degree of correlation. Here we construct such graph simply by computing pairwise Pearson correlation from empirical data, and linking two nodes if their correlation is above a given threshold ρ . Let r_{ab} denotes the weight of edge $e = (a, b) \in E$ which measures the correlation between trait a and b . Based on this graph, we can define $\Phi(\boldsymbol{\beta})$ as Equation 5:

$$\Phi(\boldsymbol{\beta}) = \lambda \|\boldsymbol{\beta}\|_1 + \gamma \sum_{e=(a,b) \in E} |r_{ab}| \sum_{i=1}^m |\boldsymbol{\beta}_a^i - \text{sign}(r_{ab})\boldsymbol{\beta}_b^i| \quad (5)$$

Where λ controls the overall sparsity and γ controls the trait dependency. Increasing the value of γ will make the correlated traits more likely to share a common set of causal SNPs. Substituting Equation 5 into Equation 3, we can get the optimization equation for the proposed sGLMM.

2.3 Parameter Inference

Optimizing the hyper-parameter $\Theta = \{\sigma_g^2, \sigma_\epsilon^2, \lambda, \gamma\}$ is a NP-hard problem. Following the algorithm described in Rakitsch *et al*, we tune σ_g^2 and σ_ϵ^2 first without SNP effect, then reduce the problem to a standard graph lasso regression problem. Such procedure has been widely used in the single-SNP mixed models and shown the similar performance compared with an exact manner (Kang *et al.*, 2010).

2.3.1 Null model fitting

To begin with, we first optimize σ_g^2 and σ_ϵ^2 without the effect of $\boldsymbol{\beta}$. Instead of tuning σ_g^2 and σ_ϵ^2 respectively, we optimize the ratio of them (Lippert *et al.*, 2011), $\delta = \sigma_\epsilon^2 / \sigma_g^2$:

$$\ell_{null}(\sigma_g, \delta) = e^{-\Phi(\boldsymbol{\beta})} \cdot \prod_{i=1}^k \mathcal{N}(\mathbf{y}_i | \mathbf{X}\boldsymbol{\beta}_i, \sigma_g^2(\mathbf{K} + \delta \mathbf{I})) \quad (6)$$

In general, we first compute the spectral decomposition of $\mathbf{K} = \mathbf{U} \text{diag}(\mathbf{d}) \mathbf{U}^T$, where \mathbf{U} for eigenvector matrix and $\text{diag}(\mathbf{d})$ for eigenvalue matrix. After that we reweigh the data to make the covariance of the Gaussian distribution isotropic. Then, we carry out a one-dimension optimization with regard to δ to optimize the log-likelihood, while σ_g can be optimized in closed form during each evaluation.

2.3.2 Reduction to standard graph-guided fused lasso

Having the resulting optimized δ and σ_g , we utilize the eigen decomposition of \mathbf{K} again to reweigh the data such that the covariance matrix becomes isotropic:

$$\tilde{\mathbf{X}} = (\text{diag}(\mathbf{d}) + \delta \mathbf{I})^{-\frac{1}{2}} \mathbf{U}^T \mathbf{X}$$

$$\tilde{\mathbf{y}}_i = (\text{diag}(\mathbf{d}) + \delta \mathbf{I})^{-\frac{1}{2}} \mathbf{U}^T \mathbf{y}_i$$

Where $\tilde{\mathbf{y}}_i$ denotes the rescaled phenotypes and $\tilde{\mathbf{X}}$ for genotypes. After that, Equation 3 can be rewritten as Equation 7:

$$\ell_{reweighed}(\boldsymbol{\beta}) = e^{-\Phi(\boldsymbol{\beta})} \cdot \prod_{i=1}^k \mathcal{N}(\tilde{\mathbf{y}}_i | \tilde{\mathbf{X}}\boldsymbol{\beta}_i, \sigma_g^2 \mathbf{I}) \quad (7)$$

After such transformation, the task is equivalent to the standard graph-structured regression model:

$$\hat{\boldsymbol{\beta}} = \min_{\boldsymbol{\beta}} \frac{1}{\sigma_g^2} \|\tilde{\mathbf{y}} - \tilde{\mathbf{X}}\boldsymbol{\beta}\|_F^2 + \Phi(\boldsymbol{\beta}) \quad (8)$$

Here, $\|\cdot\|_F$ denotes the matrix Frobenius norm, and Φ is determined by Equation 5. To solve this problem efficiently, we employ the smoothing proximal gradient descent method (Chen *et al.*, 2012).

3 Simulation study

In this section, we evaluate the performance of the proposed sGLMM model against vanilla sparse linear mixed models as well as other classical variable selection methods.

3.1 Data generation

To get the appropriate dataset with the relatedness of genes and population structure, we break the generation into three steps: generation of 1) SNPs 2) effect size matrix and 3) phenotypes.

Generation of SNPs To begin with, we need to generate the SNPs originated from g different populations. We use c_i to symbolize the centroid of the i -th population, $i = 1, \dots, g$. First, we generate centroids of g different distributions, and then SNP data from a multivariate Gaussian distribution as follows:

$$x_i \sim \mathcal{N}(c_j, \sigma_s^2 \mathbf{I})$$

where x_i denotes the i -th individual originated from j -th distribution and σ_s^2 controls the magnitude of covariance of subpopulation. Decreasing σ_s will result in stronger population structure.

Generation of effect size matrix We generate the effect size matrix $\boldsymbol{\beta}_k$ such that the output traits are correlated in a block-like structure. The generated traits are divided into g_{num} clusters in the experiment, and each cluster shares a common set of relevant SNPs. Another set of active SNPs is added to the first two clusters, simulating the situation of a higher-level correlation structure. In the end, the rows and columns are reordered randomly. An illustrative example was generated and demonstrated in Figure S1.

Generation of phenotypes We then generate a $n \times k$ intermediate output r from \mathbf{X} using the usual linear regression model:

$$r = \mathbf{X}\boldsymbol{\beta} + \epsilon$$

Here $\boldsymbol{\beta}$ is the resulting sparse matrix indicating which SNP in \mathbf{X} influences the gene expression r and $\epsilon \sim \mathcal{N}(0, \sigma_\epsilon^2 \mathbf{I})$. Since the generated $\boldsymbol{\beta}$ is correlated, the block-like structure dependency will be passed to the r automatically.

Table 1. Default parameter setting in the simulation study.

| Parameter | Default | Description |
|--------------|---------|--|
| n | 1000 | the number of samples |
| m | 5000 | the number of SNPs |
| k | 50 | the number of traits |
| d | 10% | the percentage of active SNPs |
| g | 5 | the number of subpopulations |
| g_{num} | 3 | the number of correlated trait clusters |
| σ_s^2 | 0.005 | the magnitude of covariance of subpopulations |
| σ_t^2 | 100 | the magnitude of covariance of traits caused by genetic effect |
| σ_m^2 | 0.001 | the magnitude of covariance of traits caused by shared signals |
| σ_e^2 | 50 | the magnitude of covariance of noise |

After that, to simulate a scenario with confounding factors, we introduce a covariance matrix to simulate correlations between the traits:

$$t_i \sim \mathcal{N}(r_i, \sigma_t^2 M)$$

where t is a $n \times k$ intermediate output and M is the covariance between traits caused by population structure and σ_t^2 is a scalar that controls the magnitude of covariance. Letting C be the matrix formed by stacking the centroid of each individual, we choose $M = CC^T$. This has the desired effect of making observations from the same population more correlated.

In the end, to simulate the correlation between traits caused by the shared signals, we introduce one more covariance between traits. Each row of final trait matrix can be expressed as:

$$y^i \sim \mathcal{N}(t^i, \sigma_m^2 S)$$

where S measures the covariance between traits caused by shared signals and σ_m^2 is a scalar that controls the magnitude. Here we let $S = \beta^T \beta$, which has the desired effect of making dependent traits to be more correlated.

3.2 Experimental results

The default parameters we used in our simulations are listed in Table 1. We adjust each of these 10 parameters to evaluate the performance of our model under different circumstances. We tested the proposed model as well as the following models:

- lasso, the most classical regression method used in variable selection (Tibshirani, 1996).
- SCAD (smoothly clipped absolute deviation), a method which provides continuity, sparsity, and unbiasedness by using a symmetric, nonconcave penalty (Fan and Li, 2001).
- GFlasso (graph-guided fused lasso), a multi-task regression method that incorporates the dependency information as a graph (Chen *et al.*, 2010).
- FaST-LMM-Select, an approach which considers a small number of SNPs systematically to improve its performance (Listgarten *et al.*, 2012).
- BOLT, a model which utilizes more realistic, non-infinitesimal genetic architectures to reduce the needed iteration and increase linkage power (Loh *et al.*, 2015).
- sLMM (sparse linear mixed model), a mixed model that allows for both multi-locus mapping and correction for confounding effect (Rakitsch *et al.*, 2013).

- MCP (minimax concave penalty), a method that provides fast, continuous, nearly unbiased and accurate variable selection (Zhang *et al.*, 2010b).

The results are shown as receiver operating characteristic (ROC) curves in Figure 2. The problem can be regarded as classification problem—identifying the active genetic variants from all genes. For better clarity, here we only show the low false positive rate (FPR) part of ROC curves in some experimental settings. The full ROC curves for all experimental settings are in Figure S3 and share the same pattern. The precision-recall curves are displayed in Figure S4. For each setting tested, we generated different data by ten random seeds and then drew the overall results. We also show that sGLMM’s ability to reconstruct the traits relatedness is better than GFlasso in Figure S2.

In general, the proposed sGLMM model behaves better than the other approaches in all parameter settings. FaST-LMM-Select, sLMM and GFlasso can extract some meaningful information while other traditional methods could barely find correct genetic variation throughout the whole experiment. The failure of these models proves the importance of modeling multi-source correlation in the data. As the percentage of active SNPs decreases in Figure 2d, the problem becomes less challenging, and all models behave better in a certain degree (it is the only setting where FaST-LMM-Select works), while sGLMM can keep efficient even when the training set is extremely deficient (5000 SNPs with only 500 samples). Moreover, as illustrated in Figure 2c and Figure S3f, sGLMM shows its capability of handling traits relatedness pattern in different settings. Manipulating magnitude of confounding and trait dependency as in Figure 2e, Figure S3h and Figure S3i, we notice that GFlasso and sLMM behave well only when they model the major source of correlation. For example, in Figure 2e where $\sigma_s^2 = 0.05$, GFlasso can behave as well as sGLMM, but when $\sigma_s^2 = 0.0005$, GFlasso is much worse than sGLMM due to stronger population structure. By contrast, sGLMM can keep stable performance in all settings through modeling multi-source correlation automatically. Interestingly, sLMM’s ROC curve coincides in part with our proposed model, suggesting these two models attach the biggest effect size to the same set of SNPs. However, the sGLMM overshadows sLMM by capturing the weak association in the data through utilizing the relatedness information.

4 Real genome data experiment

Having shown the efficiency of sGLMM in simulated datasets, we now demonstrate the proposed model is also an effective method in real datasets.

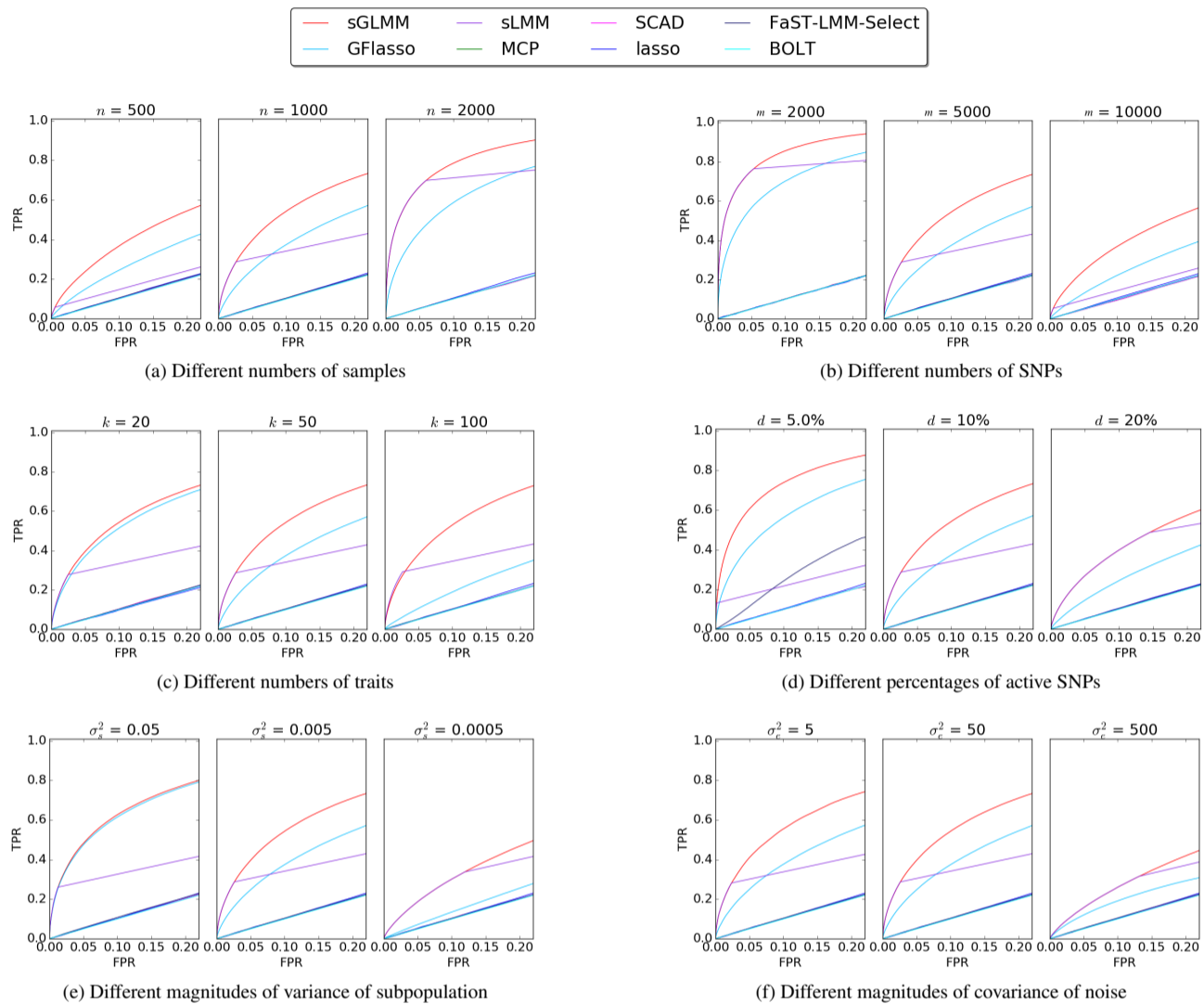


Fig. 2. Receiver operating characteristic (ROC) curves for experiments with various parameters. We show low FPR part of ROC curves to compare our method with existing methods. For each configuration, the reported curve is drawn over ten random seeds.

To evaluate the method, we identify genetic variants in Alzheimer’s disease (AD) and Arabidopsis thaliana, and then we evaluate our findings with the published results in relevant literature to show the reliability of our methods compared with existing approaches. The details of preprocessing the data are described in Supplementary data.

4.1 Data Sets

4.1.1 Arabidopsis thaliana

The Arabidopsis thaliana dataset we obtained is a collection of around 200 plants, each with around 215,000 genetic variables (Anastasio *et al.*, 2011). We identified the causal genetic variables of 44 observed traits such as days to germination, days to flowering, lesioning, etc. These plants were distributed from 27 different countries in Europe and Asia, resulting in a potential confounding factor. For instances, different geographic origins may have different moisture and air conditions, which could affect the observed traits of the plants. Besides there are some correlated traits such as FT10, FT16 and FT20, which measure the flowering time in different temperature.

4.1.2 Alzheimer’s disease

We use the late-onset Alzheimer’s disease data provided by Harvard Brain Tissue Resource Center and Merck Research Laboratories (Zhang *et al.*, 2013). It consists of measurements of 540 patients with 500,000 genetic variables. We tested the association between these SNPs and 28 phenotypes corresponding to a patient’s disease status of Alzheimer’s disease.

4.2 Arabidopsis thaliana

Since we have access to a validated gold standard of Arabidopsis thaliana dataset, we could directly assess their performance by ROC curve, the same metric used in the simulation study.

Figure 3 illustrates the area under the ROC curve (AuROC) according to different traits. Generally speaking, our approach proves itself well suited to the real-world genomic dataset and outperforms all other methods for 63.4% traits. The overall average AuROC of proposed sGLMM is 0.96, while the other models’ are lower than 0.78. Since there should be some traits not suffering from the confounders, it is barely surprising that the traditional methods (e.g., MCP, GFlasso, SCAD) behave well in this case. For example, the phenotypes beginning with “FT” like FT10

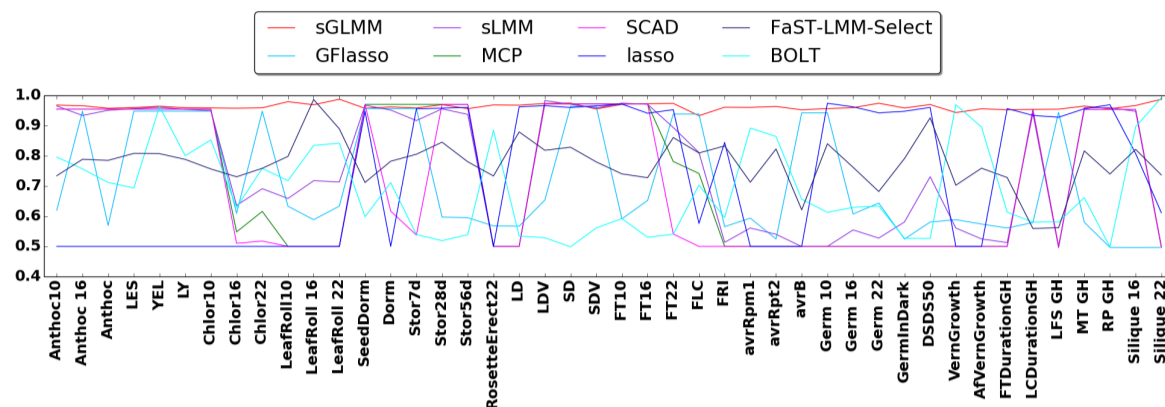


Fig. 3. Area under ROC curve (AuROC) for the 44 traits of *Arabidopsis thaliana*. For each trait, we calculate the AuROC by comparing the yielded genetic variables with the gold standard and plot the performance of each model

measure the average flowering time of days and the following numbers denote the environmental temperature. In these case, the time of daylight and temperature are rigorously controlled. As a result, the confounding introduced by the geographic origin is weakened.

4.3 Alzheimer's disease

We list the ten most significant SNPs among all 28 phenotypes found by our model in Table 2 and validate their potential association with Alzheimer's disease with previous research report.

To evaluate the accuracy of our model, here we justify SNPs discovered by our model. The 1st discovered SNP is corresponded to *C4orf50* gene, which can influence tissue-restricted expression level for the brain (Delgado *et al.*, 2014). Both the 2nd and 4th are associated with *MACROD2* gene. *MACROD2* is expressed in the brain and associated with disorders such as autism (Anney *et al.*, 2010), which is also reported to be associated with Alzheimer's disease by other model (Kohannim *et al.*, 2012). The 5th and 6th are expressed by the *TENM1* gene, which codes the Teneurin Transmembrane Protein. This protein helps to build appropriate patterns of neural connectivity, playing a crucial role in visual, olfactory and motor systems (Leamey and Sawatari, 2014; Alkelai *et al.*, 2016). The 8th SNP is associated with *CD70* gene, which is surface molecules expressed by Mature T-cells (Romero *et al.*, 2007; Salaun *et al.*, 2011). Biologists have found that the level of T-cells in AD brain is much higher than in unaffected patients (Sardi *et al.*, 2011; Song and Lee, 2015).

5 Discussion

The computational complexity of the two-stage algorithm mainly depends on the optimization of GFlasso regression. The difference between our method and graph-guided fused lasso regression is $O(n^3)$ for decomposition of \mathbf{K} , $O(n^2m + nmk)$ for reweighing the phenotype matrix \mathbf{y} and genotypes \mathbf{X} (computing $\mathbf{U}^T\mathbf{y}$ and $\mathbf{U}^T\mathbf{X}$), and $O(nmk)$ for execution of the log likelihood in the one-dimensional optimization over δ for constant times.

Our model has been implemented in Python and is free available. Currently, it supports both csv and plink format files. You can either specify the hyper-parameters or provide the program with the number of selected SNPs, otherwise the program will execute the cross validation. The detailed instruction is described in the Appendix.

In this paper, we apply a simple strategy to construct dependency graph G . However, sGLMM itself does not specify how G is obtained, so other more sophisticated approaches may be used.

6 Conclusion

In this article, we address the challenging problem in genome-wide association studies, exploring the genetic association where the data is non-i.i.d. and traits involve complex relatedness. There have been a wealth of attempts to utilize the advantages of LMM while losing sight of the interdependency among the traits. The method like graph-guided fused lasso enables the analysts to learn SNPs with pleiotropic effects that influence the activities of multiple co-expressed genes.

To solve this problem, we proposed the sparse graph-structured linear mixed model for genetic association. Our method not only corrects the irrelevant confounding but also utilizes the information of the relatedness of phenotypes into statistical analysis. We have shown that the traditional graph lasso can easily fall into the trap of utilizing false dependency information due to the confounding and using linear mixed model alone fails to capture the complex phenotypic architecture. In comparison to these approaches, sGLMM combines the advantages of both methods and remains computationally efficient. Through extensive experiments on both synthetic and real datasets, we exhibit sGLMM has a clear superiority over existing methods.

Acknowledgments

We would like to thank Haohan Wang and Eric Xing for the great insight. We also appreciate Zhou Fang for providing computational resource for some of the experiments.

Table 2. Discovered SNPs related to Alzheimer's disease.

| Rank | SNP | Chr | Chr Position | RefSNP Alleles | MAF | Gene |
|------|------------|-----|--------------|----------------|--------|---------|
| 1 | rs9999966 | 4 | 5925628 | C/T | 0.0807 | C4orf50 |
| 2 | rs16994889 | 20 | 14746661 | A/G | 0.0791 | MACROD2 |
| 3 | rs1699451 | 7 | 69288571 | A/G | 0.3908 | |
| 4 | rs16994542 | 20 | 14409645 | A/C | 0.2764 | MACROD2 |
| 5 | rs16994557 | X | 125041417 | C/T | 0.2238 | TENM1 |
| 6 | rs16994560 | X | 125047265 | C/T | 0.0816 | TENM1 |
| 7 | rs16994583 | X | 148473389 | A/G | 0.0321 | |
| 8 | rs16994592 | 19 | 6586487 | C/T | 0.0775 | CD70 |
| 9 | rs16994602 | 4 | 38536223 | A/C/G | 0.1492 | |
| 10 | rs1699463 | 9 | 23853359 | A/G | 0.4139 | |

References

- Alkelai, A., Olender, T., Haffner-Krausz, R., Tsoory, M., Boyko, V., Tatarkyy, P., Gross-Isseroff, R., Milgrom, R., Shushan, S., Blau, I., *et al.* (2016). A role for *tenm1* mutations in congenital general anosmia. *Clinical genetics*, **90**(3), 211–219.
- Anastasio, A. E., Platt, A., Horton, M., Grotewold, E., Scholl, R., Borevitz, J. O., Nordborg, M., and Bergelson, J. (2011). Source verification of mis-identified *Arabidopsis thaliana* accessions. *The Plant Journal*, **67**(3), 554–566.
- Anney, R., Klei, L., Pinto, D., Regan, R., Conroy, J., Magalhaes, T. R., Correia, C., Abrahams, B. S., Sykes, N., Pagnamenta, A. T., *et al.* (2010). A genome-wide scan for common alleles affecting risk for autism. *Human molecular genetics*, **19**(20), 4072–4082.
- Astle, W. and Balding, D. J. (2009). Population structure and cryptic relatedness in genetic association studies. *Statistical Science*, pages 451–471.
- Bondell, H. D., Krishna, A., and Ghosh, S. K. (2010). Joint variable selection for fixed and random effects in linear mixed-effects models. *Biometrics*, **66**(4), 1069–1077.
- Chen, X., Kim, S., Lin, Q., Carbonell, J. G., and Xing, E. P. (2010). Graph-structured multi-task regression and an efficient optimization method for general fused lasso. *arXiv preprint arXiv:1005.3579*.
- Chen, X., Lin, Q., Kim, S., Carbonell, J. G., and Xing, E. P. (2012). Smoothing proximal gradient method for general structured sparse regression. *The Annals of Applied Statistics*, pages 719–752.
- Craddock, N., Hurles, M. E., Cardin, N., Pearson, R. D., Plagnol, V., Robson, S., Vukcevic, D., Barnes, C., Conrad, D. F., Giannoulata, E., *et al.* (2010). Genome-wide association study of CNVs in 16,000 cases of eight common diseases and 3,000 shared controls. *Nature*, **464**(7289), 713–720.
- Delgado, A., Brandao, P., and Narayanan, R. (2014). Diabetes associated genes from the dark matter of the human proteome. *MOJ Proteomics Bioinform*, **1**(4), 00020.
- Dinga, R., Schmaal, L., Penninx, B. W., Veltman, D. J., and Marquand, A. F. (2020). Controlling for effects of confounding variables on machine learning predictions.
- Fan, J. and Li, R. (2001). Variable selection via nonconcave penalized likelihood and its oracle properties. *Journal of the American statistical Association*, **96**(456), 1348–1360.
- Fan, Y. and Li, R. (2012). Variable selection in linear mixed effects models. *Annals of statistics*, **40**(4), 2043.
- Goddard, M. (2009). Genomic selection: prediction of accuracy and maximisation of long term response. *Genetica*, **136**(2), 245–257.
- Goddard, M. E., Wray, N. R., Verbyla, K., Visscher, P. M., *et al.* (2009). Estimating effects and making predictions from genome-wide marker data. *Statistical Science*, **24**(4), 517–529.
- Hatoum, A. S., Wendt, F. R., Galimberti, M., Polimanti, R., Neale, B., Kranzler, H. R., Gelernter, J., Edenberg, H. J., and Agrawal, A. (2020). Ancestry may confound genetic machine learning: Candidate-gene prediction of opioid use disorder as an example.
- Hayeck, T. J., Zaitlen, N. A., Loh, P.-R., Vilhjalmsón, B., Pollack, S., Gusev, A., Yang, J., Chen, G.-B., Goddard, M. E., Visscher, P. M., *et al.* (2015). Mixed model with correction for case-control ascertainment increases association power. *The American Journal of Human Genetics*, **96**(5), 720–730.
- Hayes, B. J., Visscher, P. M., and Goddard, M. E. (2009). Increased accuracy of artificial selection by using the realized relationship matrix. *Genetics research*, **91**(01), 47–60.
- Hoggart, C. J., Whittaker, J. C., De Iorio, M., and Balding, D. J. (2008). Simultaneous analysis of all SNPs in genome-wide and re-sequencing association studies. *PLoS Genet*, **4**(7), e1000130.
- Kang, H. M., Zaitlen, N. A., Wade, C. M., Kirby, A., Heckerman, D., Daly, M. J., and Eskin, E. (2008). Efficient control of population structure in model organism association mapping. *Genetics*, **178**(3), 1709–1723.
- Kang, H. M., Sul, J. H., Service, S. K., Zaitlen, N. A., Kong, S.-y., Freimer, N. B., Sabatti, C., Eskin, E., *et al.* (2010). Variance component model to account for sample structure in genome-wide association studies. *Nature genetics*, **42**(4), 348–354.
- Kim, B., Shah, J. A., and Doshi-Velez, F. (2015). Mind the gap: A generative approach to interpretable feature selection and extraction. In *Advances in Neural Information Processing Systems*, pages 2260–2268.
- Kohannim, O., Hibar, D. P., Stein, J. L., Jahanshad, N., Hua, X., Rajagopalan, P., Toga, A. W., Jack Jr, C. R., Weiner, M. W., De Zubicaray, G. I., *et al.* (2012). Discovery and replication of gene influences on brain structure using lasso regression. *Frontiers in neuroscience*, **6**.
- Korte, A., Vilhjalmsón, B. J., Segura, V., Platt, A., Long, Q., and Nordborg, M. (2012). A mixed-model approach for genome-wide association studies of correlated traits in structured populations. *Nature genetics*, **44**(9), 1066–1071.
- Kruuk, L. E. (2004). Estimating genetic parameters in natural populations using the ‘animal model’. *Philosophical Transactions of the Royal Society of London B: Biological Sciences*, **359**(1446), 873–890.
- Leamey, C. A. and Sawatari, A. (2014). The teneurins: new players in the generation of visual topography. In *Seminars in cell & developmental biology*, volume 35, pages 173–179. Elsevier.
- Lippert, C., Listgarten, J., Liu, Y., Kadie, C. M., Davidson, R. I., and Heckerman, D. (2011). Fast linear mixed models for genome-wide association studies. *Nature methods*, **8**(10), 833–835.
- Listgarten, J., Lippert, C., Kadie, C. M., Davidson, R. I., Eskin, E., and Heckerman, D. (2012). Improved linear mixed models for genome-wide association studies. *Nature methods*, **9**(6), 525–526.
- Liu, X., Wang, H., Ye, W., and Xing, E. P. (2017). Sparse variable selection on high dimensional heterogeneous data with tree structured responses. *arXiv preprint arXiv:1711.08265*.
- Logsdon, B. A., Hoffman, G. E., and Mezey, J. G. (2010). A variational bayes algorithm for fast and accurate multiple locus genome-wide association analysis. *BMC bioinformatics*, **11**(1), 58.
- Loh, P.-R., Tucker, G., Bulik-Sullivan, B. K., Vilhjalmsón, B. J., Finucane, H. K., Salem, R. M., Chasman, D. I., Ridker, P. M., Neale, B. M., Berger, B., *et al.* (2015). Efficient bayesian mixed-model analysis increases association power in large cohorts. *Nature genetics*, **47**(3), 284–290.
- McCarthy, M. I., Abecasis, G. R., Cardon, L. R., Goldstein, D. B., Little, J., Ioannidis, J. P., and Hirschhorn, J. N. (2008). Genome-wide association studies for complex traits: consensus, uncertainty and challenges. *Nature reviews genetics*, **9**(5), 356–369.
- Meyer, K., Johnston, D. J., and Graser, H.-U. (2004). Estimates of the complete genetic covariance matrix for traits in multi-trait genetic evaluation of australian hereford cattle. *Crop and Pasture Science*, **55**(2), 195–210.
- Patterson, N., Price, A. L., and Reich, D. (2006). Population structure and eigenanalysis. *PLoS genet*, **2**(12), e190.
- Pirinen, M., Donnelly, P., Spencer, C. C., *et al.* (2013). Efficient computation with a linear mixed model on large-scale data sets with applications to genetic studies. *The Annals of Applied Statistics*, **7**(1), 369–390.
- Price, A. L., Patterson, N. J., Plenge, R. M., Weinblatt, M. E., Shadick, N. A., and Reich, D. (2006). Principal components analysis corrects for stratification in genome-wide association studies. *Nature genetics*, **38**(8), 904–909.
- Price, A. L., Zaitlen, N. A., Reich, D., and Patterson, N. (2010). New approaches to population stratification in genome-wide association studies. *Nature Reviews Genetics*, **11**(7), 459–463.

- Rakitsch, B., Lippert, C., Stegle, O., and Borgwardt, K. (2013). A lasso multi-marker mixed model for association mapping with population structure correction. *Bioinformatics*, **29**(2), 206–214.
- Romero, P., Zippelius, A., Kurth, I., Pittet, M. J., Touvrey, C., Iancu, E. M., Corthesy, P., Devevre, E., Speiser, D. E., and Rufer, N. (2007). Four functionally distinct populations of human effector-memory cd8+ t lymphocytes. *The Journal of Immunology*, **178**(7), 4112–4119.
- Salaun, B., Yamamoto, T., Badran, B., Tsunetsugu-Yokota, Y., Roux, A., Baitsch, L., Rouas, R., Fayyad-Kazan, H., Baumgaertner, P., Devevre, E., et al. (2011). Differentiation associated regulation of microRNA expression in vivo in human cd8+ t cell subsets. *Journal of translational medicine*, **9**(1), 44.
- Sardi, F., Fassina, L., Venturini, L., Inguscio, M., Guerriero, F., Rolfo, E., and Ricevuti, G. (2011). Alzheimer's disease, autoimmunity and inflammation. the good, the bad and the ugly. *Autoimmunity reviews*, **11**(2), 149–153.
- Segura, V., Vilhjálmsson, B. J., Platt, A., Korte, A., Seren, Ú., Long, Q., and Nordborg, M. (2012). An efficient multi-locus mixed-model approach for genome-wide association studies in structured populations. *Nature genetics*, **44**(7), 825–830.
- Song, J. and Lee, J. E. (2015). mir-155 is involved in alzheimer's disease by regulating t lymphocyte function. *Frontiers in aging neuroscience*, **7**.
- Tibshirani, R. (1996). Regression shrinkage and selection via the lasso. *Journal of the Royal Statistical Society. Series B (Methodological)*, pages 267–288.
- Visscher, P. M., Brown, M. A., McCarthy, M. I., and Yang, J. (2012). Five years of gwas discovery. *The American Journal of Human Genetics*, **90**(1), 7–24.
- Wang, H. and Yang, J. (2016). Multiple confounders correction with regularized linear mixed effect models, with application in biological processes. *bioRxiv*, page 089052.
- Wang, H., Yue, T., Yang, J., Wu, W., and Xing, E. P. (2019). Deep mixed model for marginal epistasis detection and population stratification correction in genome-wide association studies. *BMC Bioinformatics*, **20**(S23).
- Wang, H., Aragam, B., and Xing, E. P. (2022). Trade-offs of linear mixed models in genome-wide association studies. *Journal of Computational Biology*, **29**(3), 233–242.
- Wang, J., Fujimaki, R., and Motohashi, Y. (2015). Trading interpretability for accuracy: Oblique treed sparse additive models. In *Proceedings of the 21th ACM SIGKDD International Conference on Knowledge Discovery and Data Mining*, pages 1245–1254. ACM.
- Wu, T. T., Chen, Y. F., Hastie, T., Sobel, E., and Lange, K. (2009). Genome-wide association analysis by lasso penalized logistic regression. *Bioinformatics*, **25**(6), 714–721.
- Yang, J., Benyamin, B., McEvoy, B. P., Gordon, S., Henders, A. K., Nyholt, D. R., Madden, P. A., Heath, A. C., Martin, N. G., Montgomery, G. W., et al. (2010). Common snps explain a large proportion of the heritability for human height. *Nature genetics*, **42**(7), 565–569.
- Zhang, B., Gaiteri, C., Bodea, L.-G., Wang, Z., McElwee, J., Podtelezhnikov, A. A., Zhang, C., Xie, T., Tran, L., Dobrin, R., et al. (2013). Integrated systems approach identifies genetic nodes and networks in late-onset alzheimer's disease. *Cell*, **153**(3), 707–720.
- Zhang, C.-H. et al. (2010a). Nearly unbiased variable selection under minimax concave penalty. *The Annals of statistics*, **38**(2), 894–942.
- Zhang, Z., Ersoz, E., Lai, C.-Q., Todhunter, R. J., Tiwari, H. K., Gore, M. A., Bradbury, P. J., Yu, J., Arnett, D. K., Ordovas, J. M., et al. (2010b). Mixed linear model approach adapted for genome-wide association studies. *Nature genetics*, **42**(4), 355–360.